

# Evaluation of the Energy Dissipation on Composite Plates Under Conditions of Piercing Shot

Alfredo Maria Cardoso de Meneses Maldonado Passanha  
alfredo.passanha@tecnico.ulisboa.pt

Instituto Superior Técnico, Universidade de Lisboa, Portugal

December 2021

## Abstract

Ballistic protection is one of the key elements of individual security in combat. Innovation in the field of materials, combined with the complexity of analyzing ballistic impacts, leads to the development of new theoretical and experimental methodologies for the characterization of the ballistic properties of protective elements. The present investigation was focused on the development of an experimental methodology, analytically complemented, to evaluate the performance of different materials when subjected to high-speed impacts. An apparatus was developed to carry out high-speed ballistic tests, under controlled laboratory conditions, with the possibility of varying the speed, geometry and caliber of the projectiles, aiming at simulating combat conditions. Samples were manufactured in composite materials, varying the orientation of the fiber layers that compose them. The mechanical experiments carried out in order to characterize the laminates produced consisted of tensile test, flexural tests and Charpy impact tests. Lastly, it was intended to carry out a study of the influence that different projectile's geometries and fiber layers orientation of the composites produced have on the energy absorbed by the targets, in ballistic impacts, using the developed apparatus.

**Keywords:** Ballistics, projectile, composite materials, impact

## 1. Introduction

The evolution of ballistic protection elements has followed the progression of warfare systems and materials. New equipment development is inevitable to allow for the increase of the operative's protection level, as well as diminishing the physical and psychological wear of the operatives. The development of more effective and efficient protection elements is only possible with the evolution in the realm of materials. Nowadays, these elements are mostly composed of composite materials, that come in an enormous variety of choices, which creates the need for new theoretical and experimental methodologies for their characterization. The challenge, however, lies in reproducing different impact situations under controlled laboratory conditions, where it is possible to vary the energy and/or geometry of the projectile, measuring the physical variables throughout the tests, being that these are highly relevant for understanding the mode of dissipation of energy, allowing a quantitative analysis.

Considering the above-mentioned facts, the main purpose of this work consists of the development of a laboratory apparatus, intending to study the behavior of different composite materials when sub-

jected to projectile impacts and fragments. The apparatus will be projected to have the capacity of performing both high and low velocity ballistic impacts. To improve the testing range, the device will also be able to vary the caliber and geometry of the projectile in between tests. Subsequently, the ballistic impact on composite materials will be studied as well as the influence that different projectile geometries, velocities, and target fiber orientation have on the energy absorbed by the ballistic protection elements.

## 2. Background

This work was developed regarding experimental methodologies to study and characterize ballistic protection elements. These elements are intended to effectively and efficiently protect their users.

### 2.1. Ballistic Elements

Ballistics is the scientific field that studies all physical and chemical interactions to which a projectile is exposed, from its initial position to its penetration in various environments and objects, with the aim of studying its movement and behavior [1].

Terminal ballistics is the branch that covers the entire sequence of events that occur after the pro-

jectile hits the target, that is, the mechanical phenomena of penetration and impact [1].

The projectile is the only ammunition component that goes through the barrel and hits the target. In the present work, since the propulsion is carried out through a pneumatic cannon, the projectile is the only component of interest to study. Generally, it has certain essential characteristics:

- High density for maximum energy
- Being infusible, to prevent fusion with the barrel
- Being deformable or rigid depending on its final purpose (internal damage or perforation).

The projectile's geometry is designed considering air resistance and the type of target to be hit. Thus, there are numerous possible geometries [8].

### Ballistic Impact

A ballistic impact is a high-speed collision of a projectile on a target that is substantially denser than air, with a transfer of kinetic energy [3]. Impact phenomena are divided into classifications according to the speed at which they occur:

- *Low speed impact*:  $v < 250 \text{ m/s}$  (Deformations determined by the behavior of the target structure);
- *High speed impact*:  $0,25 \text{ km/s} < v < 2 \text{ km/s}$  (Target response located in a specific region);
- *Hyper speed impact*:  $v > 2 \text{ km/s}$  (Impact forces cause stresses with a greater order of magnitude than the strength of the materials involved)[5].

This classification has several limitations, the most significant being the fact that it does not consider the materials involved in the impact.

### Law of conservation of energy

The law of conservation of energy states that, in isolated systems, the total amount of energy remains constant over time. With this, and approximating the impact to an isolated system, it is concluded that there is energy transfer from the projectile to the target, which is influenced by the projectile-target pair and impact conditions.

### Ballistic Limit

The ballistic limit is a velocity that depends on the projectile-target pair. Three different situations can occur:

- Partial target perforation or deformation with projectile immobilization, since its kinetic energy is lower than the energy the target can absorb;
- Total target perforation with zero projectile velocity,  $V_0$  [12];
- Total target perforation, with non-zero projectile velocity since its kinetic energy is higher than the energy the target can absorb;

The velocity  $V_{50}$  is the impact speed of the projectile with a 50% probability of achieving total target perforation [13].

## 2.2. Composite Materials

### Mechanical Properties

The fiber orientation inside the matrix of these materials can be fixed or random, which influences their anisotropy. Generally, when the imposed loads are parallel to the fiber orientation, the material shows a better mechanical performance.

The fiber volume fraction, that represents the percentage of fiber volume in the entire volume of a composite material, significantly affects the material's behavior. In composites with higher volume fractions, the applied stresses are more evenly distributed while the binomial between fiber and matrix is balanced [4].

Fiber geometry influences the mechanical performance of composites. In general, composites reinforced with continuous and aligned fibers have better mechanical attributes than materials with discontinuous fibers [9].

Polymeric matrices have low mechanical strength and superior ductility when compared to fibers. Therefore, the matrix transfers the mechanical loads to the fibers and protects them from superficial damage [9]. The load transfer from the matrix to the fibers is made at the border area between them, called the interface. Thus, good adhesion at the interface is crucial in the transfer of mechanical stresses [4].

### 2.3. Typical materials used in protective elements

The search for lighter, high-performance ballistic protection elements leads to the search for materials with high ballistic-to-mass impact strength ratios [10]. This search has inevitably led to composite materials that have the capability to present mechanical properties different from traditional materials.

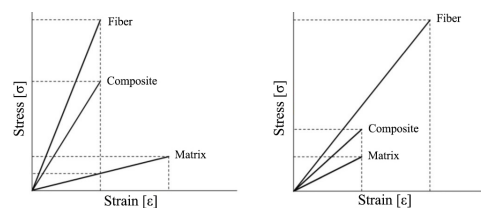


Figure 1: Stress/strain behavior of the matrix, fibers and composite. [7]

*Aramid*, marketed under the name Kevlar® , is a composite material that features great chemical, impact and fatigue characteristics as well as excellent stiffness-to-weight ratio and vibration damping capacity [6]. Due to the characteristics listed above, aramid fibers are widely used in ballistic protection elements.

*Ultra High Molecular Weight Polyethylene (UHMWPE)* composites are marketed under the names Dyneema® and Spectra® . Due to its

combination of high resistance and low density, these materials are used on a wide range of protective elements and in various other industries [2]. UHMWPE is used in ballistics, both in the form of multidirectional and unidirectional tissue [5].

*Ceramics* composites are distinguished for having greater hardness and compression resistance, when compared to the above-mentioned materials, while keeping a low density.

Nowadays, combinations of more than one of these composite materials are being studied and used for different applications.

#### 2.4. Failure Mechanisms

The manner in which targets fail when impacted by projectiles depends on the latter's mass and geometry, the impact velocity and obliqueness, the materials involved and the target's support condition [5]. In a fibrous material subjected to a ballistic impact, the fibers affected directly by projectile are called primary fibers and are subjected to the highest stresses of the process. The secondary fibers are located in the vicinity of the impact zone. These suffer generally lower deformations than the primary fibers [6]. In composite materials, some common types of failures are; rupture by delamination, matrix cracking, plugging, fiber-matrix debonding and fiber fracture, among more [5]. The transition from the target's planar geometry to a conical shape is one of the main kinetic energy transfer mechanisms of the projectile to the target [11].

#### 2.5. Ballistic Impact Analysis

The impact between projectile and the target occurs in a short period of time and involves great forces and pressures, and there may be elastic and plastic deformations in all the materials involved, so it is not an easy process to analyze. Therefore, several methods are used to study this phenomenon.

Experimental methods are performed under controlled laboratory conditions and are the main sources for validating numerical and analytical methods. But since they are destructive tests, this method is economically challenging. The analytical methods, based on the law of conservation of energy, exist in wide range of models in accordance with the selected approximations carried out [6]. The moderate simplicity of this approach allows for quick results, although not always accurate. The limitations of the methods mentioned above, create the need for new study methods. The use of numerical analysis, which presents precise results even though it also relies on approximations, has been quite common in the last two decades.

#### 2.6. Energy Balance

The kinetic energy that imposes motion on the projectile depends solely on its mass and velocity.

$$E_0^{CP} = \frac{1}{2} \times m_p \times v_0^2 \quad (1)$$

It is assumed that the impact takes place in an isolated environment, with all energy transfers occurring between the projectile and the target, and that the projectile is neither deformed nor loses mass during the process. It is possible to calculate the energy absorbed by the target during the ballistic impact, through the energy balance.

$$E_{in}^{CP} = E_r^{CP} + E^{CC} + E^{diss} \quad (2)$$

Knowing the kinetic energy values of the projectile when it hits the target ( $E_{in}^{CP}$ ) and after the impact ( $E_r^{CP}$ ), it is possible to calculate the total energy absorbed by the impacted object ( $E^{CC} + E^{diss}$ ) through the equation (2). The energy absorbed by it comprises all energy dissipation processes as well as the energy applied in the formation of the cone.

#### 2.7. Initial apparatus configuration

The ballistic testing machine initially present in the laboratory was developed in Duarte's master's thesis [8] and allowed for low-speed ballistic testing using a commercial air gun.

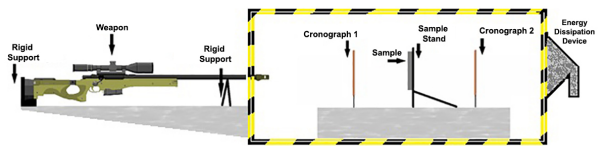


Figure 2: Initial ballistic testing machine scheme [8]

As can be seen in Figure 2, the apparatus consists of two modules, an isolated environment, called safety cage, where the impact occurs and a projectile launching system (weapon). The safety cage constituents are; ballistic windows, chronographs, a sample stand and a projectile energy dissipator [8]. This ensures that both the free movement of the projectile and the release of gases takes place entirely in the interior environment. The specimen holder allows the sample to be oriented perpendicularly to the penetration direction and the radial mobility of the fibers. The two chronographs record the incident and residual velocities of the projectiles.

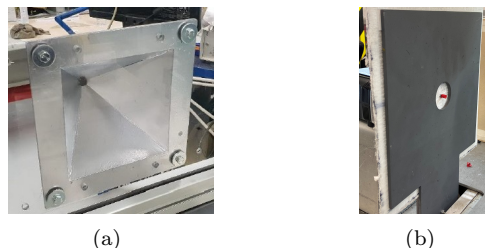


Figure 3: Energy dissipation device (EDD) interior (a) [8]; Sample stand (b)

### 3. Ballistics testing machine

#### 3.1. Security Cage Ballistic Protection Level

To carry out tests with higher energy ranges it was necessary to increase the level of ballistic protection of the cage. To do so, it was necessary to reinforce all the cage's windows as well as the EDD.

*Design of the ballistic windows:* Currently, these windows are built in asymmetric combinations of glass and polycarbonate in order to combine the properties of both materials.

To the cage windows, composed by a single acrylic plate, an additional acrylic plate was added to the inner face and a polycarbonate one to the outer face, screwed together at four points. The window where the EDD is fixed was replaced by 10, 1mm thick, steel plates as this window is subjected to direct impact from the projectile should any misalignment occur, unlike the other windows.



Figure 4: Reinforced windows profile (a); Impact window (b)

*Energy dissipation device reinforcement:* In order to reinforce this piece, several aluminum plates were joined to the device through MIG/MAG welding to guarantee the safety of the laboratorial tests.

*Other modifications:* A brake was manufactured and integrated into the structure, which prevents the cage from closing due to its own weight, for easy access to its interior.

An adapter was manufactured, as well, for the new barrels to be used, as the existence of a gap in the window-barrel interaction threatens the operator's safety. Two acrylic glass adapters were machined, for barrels with different external diameters, using a conventional lathe.

Lastly, ahead of each chronograph, two aluminum plates with an orifice, for the passage of the projectile, were introduced to protect the sensors and to reduce the displaced air's influence on the devices.

#### 3.2. Weapon Design and Manufacturing for Ballistic Tests

*Working principle:* The great challenge in the construction of the laboratory weapon was to reach speeds superior to those achieved by any commercial compressed air weapon, while also allowing for different caliber and geometry projectiles to

be used. To this end, an apparatus was designed in which the projectile is subjected to a certain amount of pressurized air, firing it through the barrel and into the target.

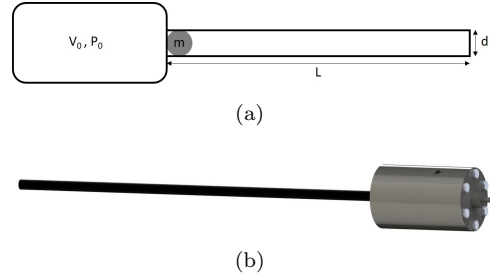


Figure 5: Weapon scheme (a) & design (b)

To analyze the parameters that influence the projectile's muzzle velocity, several assumptions were made:

- The friction of the projectile-barrel interaction is neglected;
- Uniformly accelerated rectilinear movement of the projectile, inside the barrel is assumed;
- The reduction of pressure over time and air resistance is neglected, as is any other loss of energy.;
- Total sealing is assumed in the projectile-barrel interaction, ignoring friction;

$$P = \frac{F}{A} \quad (3) \quad F = m \times a \quad (4)$$

$$L = \frac{1}{2} \times a \times t^2 \quad (5) \quad v = a \times t \quad (6)$$

Rearranging these equations, we obtain:

$$v = \frac{P \times A}{m} \sqrt{\frac{2 \times L \times m}{P \times A}} \quad (7)$$

This model allows us to conclude that the muzzle velocity of the projectile  $v$  increases proportionally with rising pressure  $P$ , projected area of the projectile  $A$  and barrel length  $L$  while it decreases with increasing projectile mass  $m$ .

*Prototype:* Analyzing the Figure 6 it is possible to observe the general working principle of the apparatus. The air reservoir (1) and its cover (2) store the pressurized air until the trigger is actuated. The punch (3) seals the air passage to the barrel (4) and, through linear motion, it has the ability to unblock this passage when the trigger is pulled.

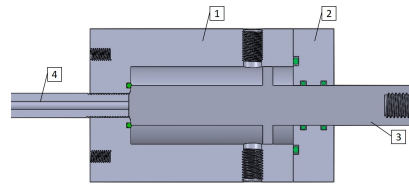


Figure 6: Prototype components

The O-rings (in green) are responsible of sealing the components. The reservoir and its cover are



coupled together using 6 M6 screws. The barrel is assembled in the apparatus through the thread at its end, which allows for the assembly of different caliber barrels.

The punch is coupled to a pneumatic actuator that launches it in its linear movement. The radial protrusion on the punch, in addition to its alignment function, acts as a stopper so that this component remains in the correct position when the apparatus is fired. The two threaded and through holes in the pressure vessel are used for the pressurization and for the introduction of a manometer for tests to be carried out in a controlled laboratory environment. The movement of the punch causes an increase in the volume of the reservoir which results in the shooting pressure to be 95% of the imposed pressure. A preload was introduced to the punch in order to prevent its movement, caused by the pressurized air molecules, without compromising its correct functioning.

*Weapon Support:* A support for the weapon was designed and manufactured with the objective of keeping it fixed and aligned with the components of the security cage.

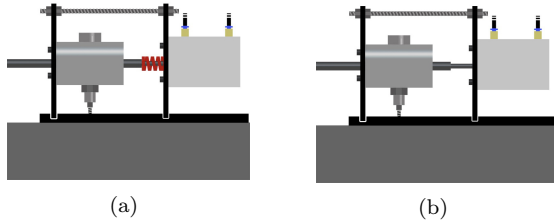


Figure 7: Weapon support scheme, with (a) and without preload (b)

The support consists of 3 metal plates, one aligned horizontally and two vertically. Two threaded rods were introduced for the connection between the vertical plates, increasing the rigidity of the support.

*Manufacturing:* The air reservoir, the cover and the punch were manufactured in the NOF laboratory using CNC milling machines. The commercially acquired barrels were threaded at their end, also in the NOF. The gun holder was manufactured using a 3-axis industrial milling machine. This operation was carried out trying to ensure the perfect alignment of the weapon. The manufacture of this support was made by reusing metal plates that were in the warehouse of the Laboratory of Machining and Micro-Manufacture of the Instituto Superior Técnico ("M3").

In order to reinforce the ballistic windows; acrylic glass and polycarbonate sheets were purchased, processed and mounted on the apparatus. Keeping the mindset of using end-of-life parts present in the laboratory, the impact window, the cage brake, the chronograph protection plates and the barrel

adapters were manufactured reusing leftover parts present in the warehouse.

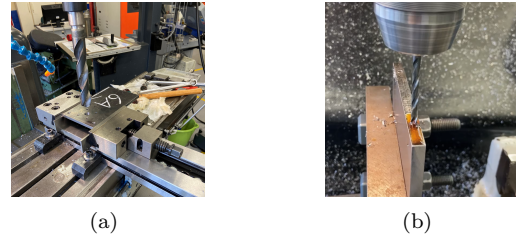


Figure 8: Weapon support manufacturing process

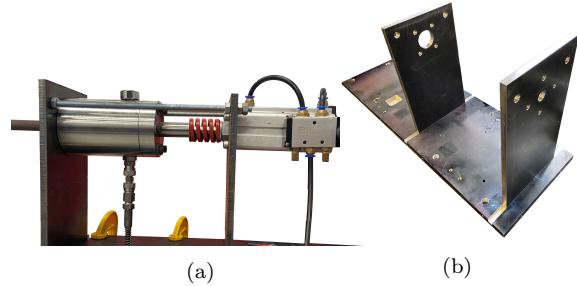


Figure 9: Developed apparatus (a); Fabricated support (b)

### 3.3. Instrumentation and Validation

#### *Ballistic Windows*

To validate the safety of the ballistic windows, a weapon was shot in a firing range at a prototype with the same configuration as the cage windows. One shot was fired with a .22 caliber gun and .22LR 40gr. Thunderbolt ammunition produced by Remington. This ammunition, with a mass of 2.59 grams, has a velocity and energy at the muzzle of 384.5 m/s and 191 J, respectively. The test was performed at a distance of 20 meters, with the projectile hitting the prototype window at a 45° inclination since, in the cage, the windows will never be subjected to a direct shot, only to ricochets.

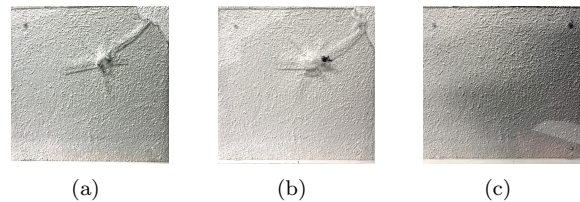


Figure 10: Ballistic window prototype after the test: acrylic glass plate where the impact occurs (a); inner acrylic glass plate (b); polycarbonate plate (c)

Regarding Figure 10, it is possible to conclude that the reinforcement of the ballistic windows was a success, since the projectile did not pass through the prototype, ensuring the safety of everyone present in the laboratory.

*Laboratory weapon:* The available equipment can reach a pressure of 200 bar. This pressurized air inside the reservoir imposes high forces on its walls

and cover, thus, class 8.8 screws were chosen in order to guarantee a safety factor greater than 4, to ensure that the device will not fail due to its fasteners.

Table 1: Projectile muzzle velocity using different work pressures

Pressure [bar]	Projectile muzzle velocity [m/s]
80	322,6
120	363,9
160	398,5

Three tests were performed at each pressure value, the projectile velocity values shown in Table 1 are the average of these. No tests were carried out using a working pressure of 200 bar as the target speed (400 m/s) was reached at a lower pressure value. These tests were carried out with a 800 mm length pipe with an internal diameter of 8 mm. The projectiles, solid steel spheres, have 7.938 mm of diameter.

As a barrel of the same caliber but of shorter length (500 mm) was acquired, tests were carried out, with the same projectiles, at 160 bar in order to verify the barrel length influence on the projectile's muzzle velocity. The velocities reached were about 330 m/s, less 70 m/s than speed reached under the same conditions with the longer barrel, which validates the conclusion from (7).

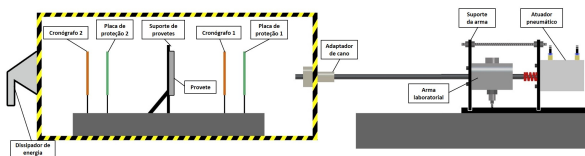


Figure 11: Layout of the laboratory machine

#### 4. Materials and Procedures

The laminates and specimens needed to carry out experimental tests were produced at Associação Fibrenamics - Instituto de Inovação em Materiais Fibrosos e Compósitos da Universidade do Minho. The experimental test carried out in order to obtain as much information as possible about their mechanical properties for later later comparison with the experimental results from the ballistic tests, were also carried at Fibrenamics.

##### 4.1. Production

To produce the laminates [0,90] fiber fabrics were used: aramid (80  $g/m^2$ ), E-glass (300  $g/m^2$ ), pre-impregnated S-glass (815  $g/m^2$ ) with 33% of epoxy matrix mass fraction and a pre-impregnated UHMWPE ( $\pm 240-271 g/m^2$ ). The tissues obtained are shown in Figure 12.

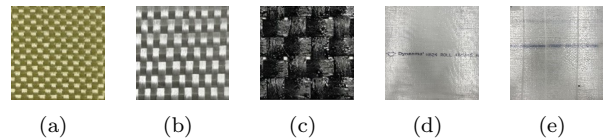


Figure 12: [0,90]° fabrics: aramid (a), E-glass (b), S-glass (c), HB24 (d) e Spectra 7727 (e)

The epoxy resin used to impregnate the fabrics was SR GreenPoxy 33 / SZ 8525.

The fabrics of each type of fiber were cut into  $250 \times 250$  mm pieces using a blade suitable for cutting fibers. The portions were cut with orientations of  $0^\circ$  and  $15^\circ$ , with the objective of producing angle-ply laminates.

The fabrics of aramid and E-glass were impregnated by hand. After processing the fabrics, they were deposited with the different orientations to produce the angle-ply laminates as shown in Figure 13.

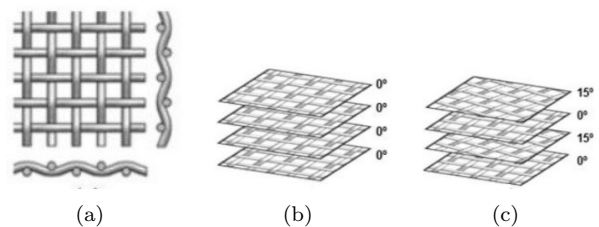


Figure 13: Fiber orientations in the produced samples: [0,90] fabrics (a), fabrics positioning  $(0,0)^\circ$  (b) and  $(0,15)^\circ$  (c)

After the impregnation process, the samples were compressed and heated in order to cure the epoxy resin and compact the fibers. A pressure of  $11 \pm 2$  bar was applied at a temperature of  $95^\circ\text{C}$  for 25 minutes. All the produced composites have a resin mass fraction of around 30%.

##### 4.2. Experimental Procedures

For the mechanical characterization of the materials to be studied, 3 tests were carried out: tensile test, flexural test and Charpy impact test.

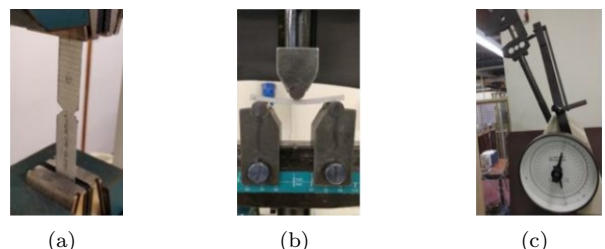


Figure 14: Mechanical tests performed: tensile (a), flexural (b) and Charpy impact (c)

The tensile tests were carried out at a speed of 1  $mm/min$  according to ISO 527-4. Six samples of each laminate were tested.

The flexural tests were performed at a speed of 2,5 mm/min in accordance with ISO 178 and were tested, as in the previous test, six samples per laminate produced.

Charpy tests were performed using a hammer with 150J of initial energy, according to ISO 179-1, on six samples of each material without a notch. Knowing the difference between initial and final energy of the hammer its possible to calculate the Charpy's impact resistance.

**Ballistic Tests:** The ballistic tests were carried out using two commercial compressed air guns (24 and 40J) and the apparatus developed in the present work.

Based on the study [8], two projectiles were chosen: Heavy Long Range Pellets (m=1.15g) and Prometheus (m=0.58g). These projectiles were chosen because, among those available at "M3" laboratory, the Prometheus are the ones with the greatest penetration power and the Heavy Pellets the ones with the greatest stopping power. Both projectiles are bi-material, with a metallic core and polymeric casing.

It is intended to use the laboratory weapon developed with a barrel of 8 mm of internal diameter and 800 mm length. The projectiles used in this weapon, for the ballistic tests, are solid steel spheres, with 7.938 mm of diameter and a mass of 2g. It is intended to operate the weapon with 160 bar of working pressure to reach velocities of about 400 m/s and obtain energies of about 160 J.

Knowing the mass and velocity that animate the projectiles, all the energies reached by them were calculated using the equation of kinetic energy (1) in subchapter 2.6.

It is proposed to carry out 5 ballistic impact tests, for each weapon-projectile combination, on the laminates produced with aramidic, E-glass and S-glass fibers. Due to the higher cost of UHMWPE laminates, it was decided to test these only using the designed laboratory weapon.

Thus, it is intended to study the influence of the projectile's geometry and velocity on ballistic impacts. It is also intended to study the different layers orientation of angle-ply structures influence when subjected to high velocity impact.

## 5. Results and discussion

### 5.1. Mechanical Tests

The mechanical tests performed to characterize the composite materials were not performed on UHMWPE laminates for the same reason that the ballistic tests using commercial airguns were not carried out on these specimens and because there is no perforation guaranteed. As the matrix used in the production of laminates is the same epoxy resin with similar mass fractions (approximately 30

to 33% of the sample mass), the difference in results between materials is associated with the mechanical properties of the fibers.

*Tensile tests:*

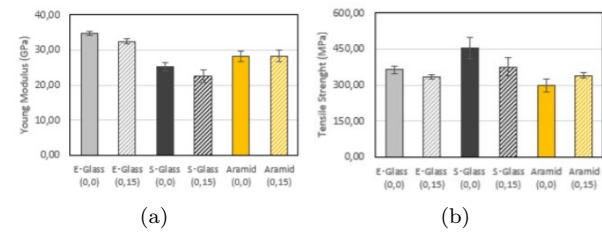


Figure 15: Obtained tensile results: Young Modulus (a) and Tensile Strength (b)

It is possible to verify, through the obtained results, that the combination of E-glass laminates presents the highest Young modulus. According to the layer orientation, it is possible to infer that the orientation  $(0,0)^\circ$  presents higher modulus values when compared to the  $(0,15)^\circ$  orientation. These results are explained by the fact that composites present better mechanical performance when the stresses are made in the alignment of the fibers. The tensile strength is higher in S-glass composites.

*Flexural tests:*

The results obtained for each combination produced are shown in Figure 16.

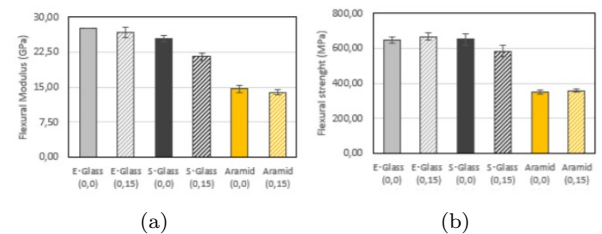


Figure 16: Obtained flexural results: Flexural modulus (a) and flexural strength (b)

According to the layers orientation, it is possible to conclude that, the laminates with orientations  $(0,0)^\circ$  present higher flexural modulus than samples with  $(0,15)^\circ$  orientations. It is observable a slight increase in the flexural strength of E-glass and aramid laminates when passing from orientations  $(0,0)^\circ$  to  $(0,15)^\circ$ , in the case of S-glass samples, the opposite is true. This indicates that the use of  $(0,15)^\circ$  orientations can positively influence the maximum stresses supported by composite structures.

*Charpy impact tests:* The analysis of the specimens after the test showed complete rupture on two of the three E-glass  $(0,0)^\circ$  samples and partial rupture with some delamination on the remaining samples of the same material and on all the S-glass

specimens tested. To the aramid samples it is also verified a partial rupture but with higher warpage when compared to the remaining laminates.

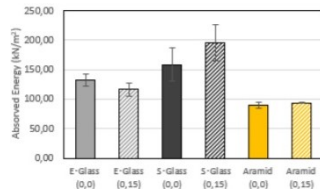


Figure 17: Obtained results for Charpy impact tests

Through the Charpy impact tests, it was verified that the combinations that absorbed the greatest impact energy were S-glass, followed by E-glass and, finally, material composed of aramid fibers. As for the layers orientation, it is easy to analyse that  $(0,15)^\circ$  orientations showed higher energy absorption on S-glass and aramid laminates while on E-glass materials the orientation  $(0,0)^\circ$  the energy absorbed is higher. The results that show advantageous mechanical properties with  $(0,15)^\circ$  orientations can be explained by the fact that the variation of the layers orientation promotes energy dissipation.

## 6. Ballistic Tests

With the commercial airguns it was not always possible to obtain results due to the characteristics of the projectiles and samples. After the ballistic impact, during some tests, there was a change in the trajectory of the projectile which prevented the recording of the residual velocity, but essentially what did not allow the measurement of useful results for the study, was the fact that the projectiles were composed by two different materials which caused them to disintegrate during the process being impossible to admit that the projectile is indeformable and maintains its mass. The tests carried out with the use of the developed weapon allowed the obtention of useful results on all the tests due to the simple projectile geometry and composition.

The obtained results were organized in two different ways:

- By sample and showing the weapon and type of projectile used, allowing the analysis of the projectiles geometry and velocity. These results show the projectiles incident and residual velocities and energies.

- By material distinguishing the laminates with different fabric layers orientation, enabling the analysis of these orientations influence on absorbed energy. These results show the values of energy absorbed by sample as a function of the projectile's incident velocity. For this analysis, only the values obtained from the tests performed with the mono-material spherical projectiles fired by the developed

apparatus were manipulated due to the simple projectile's geometry and composition.

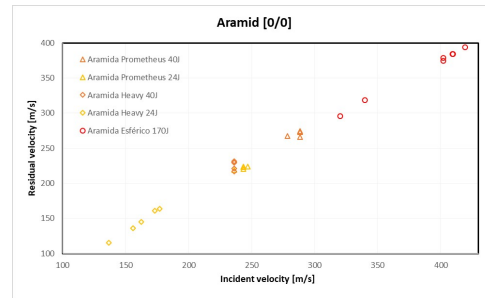


Figure 18: Incident and residual velocity results obtained for aramid laminates with  $(0,0)^\circ$  orientations

The symbols indicate the type of projectile used: triangle - Prometheus; diamond - Heavy Long Range Pellets; circumference - solid steel spheres. The colors indicate the projectile launching system used, yellow for the 24J airgun, orange for the 40J weapon and red for the developed machine. The linear evolution of the velocity and energy responses obtained is visible, suggesting that the quotient between projectiles impact and residual energies is a characteristic very influenced by the impacted target and not so much by the projectile's type and velocity, for the tested ranges. This linearity was obtained in all the tested samples and was called ballistic sample signature.

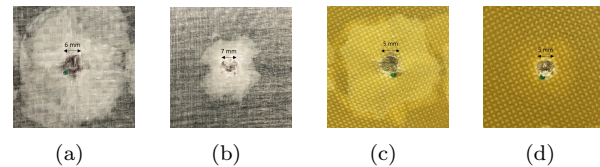


Figure 19: Entry projectile hole on aramid samples, in yellow, and on E-glass samples, in gray, at low (a),(c) and high (b),(d) velocity impacts

Figure 19 demonstrates that are associated, to high velocity impacts, responses localized in a small area while the response to low velocity impacts implies deformations in a larger area.

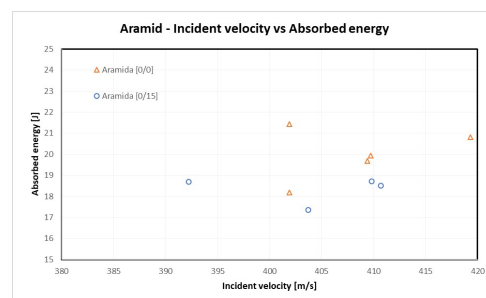


Figure 20: Absorbed energy vs incident velocity

The results organized in order to understand the influence of fiber layer orientations on the energy



absorbed by aramid samples are shown in Figure 20. The orange triangular symbols represent the results from tests performed on  $(0,0)^\circ$  laminates and the blue circular ones the results from the  $(0,15)^\circ$  samples.

In aramid combinations its observed that, in general, samples with  $(0,0)^\circ$  orientations absorbed a greater amount of kinetic energy from the projectile. Its not possible to reach any conclusion about the layers orientation, on both E and S glass combinations, perhaps due to the reduced amount of layers that compose them (6 and 2, respectively). On the UHMWPE laminates it was observed that Spectra samples absorbed a greater amount of energy on the  $(0,0)^\circ$  configuration while HB 24 samples caused greater projectile's velocity reduction on layering  $(0,15)^\circ$ . At first, the results from these two material should be similar due to the similarities of their characteristics, however, it was verified that during the spectra samples molding process the matrix did not completely melt, which may have contributed to a worse interface adhesion and different mechanical properties of the resin.

With the results obtained, it can be stated that the layer orientation influences the ballistic performance of the targets, although it is not possible to conclude generally how. However, by the analysis of the mechanical tests, it can be seen that layer orientation influences the properties studied for different materials in a different way, so it also possible that the influence of these orientations on the ballistic performance differs depending on the material.

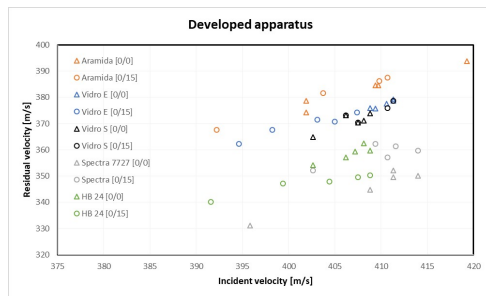


Figure 21: Incident and residual velocities obtained using the developed weapon

Analysing Figure 21 its possible to admit that the UHMWPE samples are the ones with the best ballistic performance since they are able absorb a greater amount of the projectile's kinetic energy evidenced by the larger velocity variation under the conditions of the performed tests. Already predicted from the results of the mechanical tests, the samples that showed lower ballistic protection capacity were the aramid. The E and S glass laminates exhibit very similar energy absorptions.

Figures 22 and 23 show the projectile's entry and

exit holes on the tested samples, respectively.

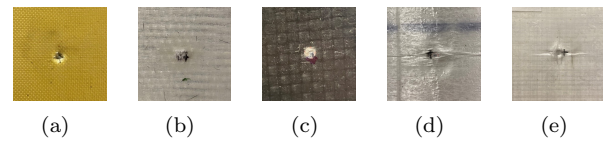


Figure 22: Projectile's entry hole: aramid (a); E-glass (b); S-glass (c); Spectra 7727 (d); HB 24 (e)

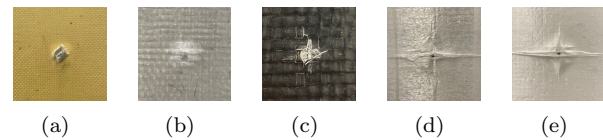


Figure 23: Projectile's exit hole: aramid (a); E-glass (b); S-glass (c); Spectra 7727 (d); HB 24 (e)

The samples condition after performing the ballistic tests allowed the energy dissipation mechanisms observation: matrix cracking, fiber rupture, interface debonding and delamination. It was also verified that the transition from the target's planar geometry to a conical shape was more accentuated on UHMWPE samples, being this energy absorption mechanism one of the reasons why these samples showed higher ballistic performance.

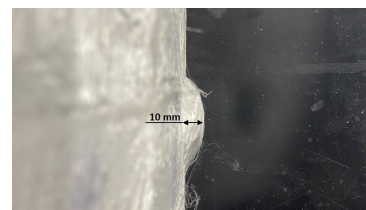


Figure 24: Conical shape on UHMWPE samples after ballistic test

## 7. Conclusions

The main objective of the dissertation, the development an apparatus to perform ballistic tests under controlled laboratory conditions with variable velocity, geometry and caliber, was achieved. The success achieved is evidenced by the fact that useful results were measured in all tests carried out using the apparatus, something that did not happen when using the compressed air guns, in addition to visible velocity performances, greater than Mach 1.

It was possible to conclude that the laminates energy absorption on high velocity impacts although dependent on the characteristics of the constituents of the projectile-target interaction is essentially influenced by characteristics of the impacted material and incident velocity since a sample ballistic signature was verified dependent on the projectile's velocity but not on its geometry.



Regarding the layers orientation influence on ballistic impact, the present investigation did not obtain results that allow a general conclusion, although it is possible to observe that certain orientations present better impact resistance depending on the composite, as is the case of  $(0,0)^\circ$  aramid fabrics that absorb higher quantity of energy than  $(0,15)^\circ$  configurations. Contrary to these results, HB 24 composites show better ballistic performance on  $(0,15)^\circ$  configurations making a conclusion about the layers orientation influence on the energy absorption embracing all the materials impossible. However, it was found that various mechanical characteristics vary as a function of layers orientation differently for different materials which may indicate that this orientation unevenly influence the ballistic performance according the laminate. The reduced number of layers on the laminates tested may not have evidenced the layers orientation influence on the ballistic impact arising the need to repeat the tests on samples with a larger number of layers.

The composites that present higher resistant projectile penetration, among those studied, are the UHMWPE composites, as they are the ones that caused larger reductions on the projectile's velocity. The aramid samples showed the worst ballistic performance.

It was also found that the greater the projectile's velocity the smaller target area is influenced by the impact waves.

As for improvements on the developed apparatus, it is suggested:

- The use of higher resistance class screws that assemble the reservoir to its cover to allow the use of higher working pressures in order to achieve higher muzzle velocities;

- The use of longer pipes also to increase the muzzle velocities;

- Computational monitoring of the working pressure value since the used manometer did not allow accurate measurements.

Regarding the study of the layers orientation influence on composites ballistic properties, it is suggested new tests carried out on laminates composed of more fabric layers covering a wide range of velocities for the same projectile's geometry and caliber.

The ability of the apparatus to vary the impact conditions was not used on the present study so it is proposed to carry out studies that make use of this skill.

It is also counseled the use of the apparatus to carry out tests that allow the study of the barrel-projectile tribological phenomena making this equipment useful for internal ballistic studies.

## References

- [1] D. E. Carlucci and S. S. Jacobson. *Ballistics: Theory and Design of Guns and Ammunition*. Taylor and Francis/CRC Press, 2007.
- [2] X. Chen. *Advanced fibrous composite materials for ballistic protection*. Woodhead Publishing, 2016.
- [3] R. M. Coupland, M. A. Rothchild, M. J. Thali, and B. P. Kneubuehl. *Wound ballistics: basics and applications*. Springer Medizin, 2011.
- [4] J. M. da Cruz Rodrigues. Desenvolvimento e fabrico de compósitos de matriz polimérica com fibras naturais. Master's thesis, Instituto Politécnico de Leiria, 2017.
- [5] J. M. C. da Fonseca Justo. Estudo do comportamento ao impacto de alta velocidade de estruturas em materiais compósitos. Master's thesis, Faculdade de Engenharia da Universidade do Porto, 1996.
- [6] J. A. da Silva Santos. Métodos de análise de impactos balísticos. Master's thesis, Faculdade de Engenharia da Universidade do Porto, 2016.
- [7] M. F. S. F. de Moura, A. B. de Morais, and A. G. de Magalhães. *Materiais Compósitos - Materiais, Fabrico e Comportamento Mecânico*. Publindústria, Edições Técnicas, 2010.
- [8] F. M. G. A. Duarte. Caracterização e modelação do comportamento de blindagens balísticas. Master's thesis, Instituto Superior Técnico, 2019.
- [9] T. F. Fernandes. Preparação e caracterização de novos materiais compósitos baseados em fibras de celulose. Master's thesis, Universidade de Aveiro, 2008.
- [10] W. Liu, Z. Chen, X. Cheng, Y. Wang, A. R. Amankwa, and J. Xu. Design and ballistic penetration of the ceramic composite armor. *Composites Part B: Engineering*, 84:33–40, 2016.
- [11] N. Naik and P. Shrirao. Composite structures under ballistic impact. *Composite Structures*, 2004.
- [12] M. Pasquali, C. Terra, and P. Gaudenzi. Analytical modelling of high-velocity impacts on thin woven fabric composite targets. *Composite Structures*, 131:951–965, 2015.
- [13] M. A. G. Silva, C. Cismasiu, and C. G. Chiorean. Numerical simulation of ballistic impact on composite laminates. *International Journal of Impact Engineering*, 2005.